Energy for Sustainable Development 70 (2022) 10–22

Contents lists available at ScienceDirect

Energy for Sustainable Development

Energy, emissions, economic analysis of air-source heat pump with radiant heating system in hot-summer and cold-winter zone in China

Qiong Chen [a,b,c], Nan Li [a,b,*]

[a] National Centre for International Research of Low-carbon and Green Buildings, Ministry of Science & Technology, Chongqing University, Chongqing 400044, China
[b] Department of Civil Engineering, Chongqing University, Chongqing 400044, China
[c] School of Civil Engineering and Architecture, Wuhan University of Technology, Wuhan 430070, China

ARTICLE INFO

Article history:
Received 17 May 2022
Revised 27 June 2022
Accepted 10 July 2022
Available online 19 July 2022

Keywords:
Air-source heat pump
Energy-saving
Economic benefit
Carbon neutrality
Radiant heating

ABSTRACT

The energy savings and economic performance study of the air-source heat pump (ASHP) and wall-hanging gas boiler (WGB) heating systems in hot-summer and cold-winter (HSCW) zones of China is beneficial to the development and implementation of relevant policies under the carbon neutrality background. This research presented a comprehensive analysis of the heat load, primary energy consumption, carbon dioxide and other emissions, and running costs of both heating systems in HSCW zones. Theoretical mathematical models of the energy consumption, emission, and economic performance of the ASHP and WGB heating systems were developed. The calculation results showed that the ASHP system consumed 12.3 % less primary energy than the WGB system, emitted 36.9 % more carbon dioxide, and reduced running costs by 26.0 %, where the increase in carbon dioxide emissions was mainly due to the limited heat-to-electricity conversion efficiency of grid systems. The experimental results showed the excellent energy consumption saving and economic benefits of the ASHP system compared to the WGB system, which promoted the applications of ASHP on a larger scale in HSCW zones of China. The comprehensive research results on the energy-saving and carbon dioxide emission performance of ASHP and WGB can contribute to evaluating the necessity of replacing WGB with ASHP and provide references for relevant policy planning in HSCW zones in China. The replacement of WGB with ASHP for spacing heating systems is promising coupled with the power system reformation to reduce carbon dioxide emissions and accomplish China's carbon neutrality target.

Introduction

The International Energy Agency (IEA) (IEA, 2020a) stated that global energy demand declined by 5 % in 2020. Renewables 2020 - Analysis and Forecast to 2025 (IEA, 2020b) predicted that renewable energy as the world's dominant source of power generation will replace coal which has ruled the world for nearly 50 years by 2025. According to BP Energy Outlook: 2020 edition (BP, 2020), the energy structure reformation for reducing the demand for fossil energy and promoting the use of renewable energy is urgent in the world. Energy-saving and carbon dioxide emission reductions are still the main research interests (Wu et al., 2020). Various countries' massive carbon dioxide emissions pose a severe threat to folks (Chen et al., 2021). China has proposed the great goal of peaking carbon dioxide emissions by 2030 and achieving carbon neutrality by 2060 (China Report, 2022). To achieve this goal, China should accelerate the energy structure reformation, and vigorous renewable energy source developments are a promising solution to carbon neutrality.

Many scholars have conducted extensive research on applying renewable energy such as ground-source heat pumps (GSHP), solar collectors, and air-source heat pumps (ASHP) (Latorre-Biel et al., 2018; Zhang et al., 2019) to significantly improve the energy efficiency of space heating systems (Cai et al., 2020; Girard et al., 2015; Pinamonti & Baggio, 2020). From the international definition of renewable energy properties (Liu et al., 2020) and the legal definition of renewable energy in China's Renewable Energy Law, air thermal energy has the same renewable energy properties as shallow geothermal energy, which has been included in the renewable energy category.

At present, various researches on energy-saving technologies and measurements for space heating systems mainly focus on the innovative heat storage materials development (Olsthoorn et al., 2017), the heat supply capacity enhancement of radiant surfaces (Ahn & Song, 2010), combination with energy-efficiency heat pump technology (Cai et al., 2021), and taking advantage of renewable energy sources such as geothermal energy, solar energy, and air thermal energy (Stetiu, 1999; Xu et al., 2010). ASHP technology (Wang et al., 2020) enables the efficient and

* Corresponding author at: National Centre for International Research of Low-carbon and Green Buildings, Ministry of Science & Technology, Chongqing University, Chongqing 400044, China.
E-mail address: nanlicqu@126.com (N. Li).

https://doi.org/10.1016/j.esd.2022.07.002

Nomenclature

Q	The primary energy consumption of heating systems, $kgce/m^2$
Q_{hl}	The heat load of the residential building, kWh/m^2
COP_{ASHP}	The coefficient of performance of ASHP
η_{gt}	The grid transmission efficiency, %
η_{ge}	The average national power generation efficiency, %
η_{ng}	The heating efficiency of the wall-hanging gas boiler, %
β_{ec}	The standard coal coefficient of electricity, 0.1229 kgce/kWh
LHV_{sc}	The lower heating value of standard coal, 29.3076 MJ/kg
LHV_{ng}	The lower heating value of natural gas, 35.59 MJ/m^3
$m_{emission}$	The total emissions per unit area, kg/m^2
m_{CO_2}	The carbon dioxide emission per unit area, kg/m^2
m_{SO_2}	The sulfur dioxide emission per unit area, kg/m^2
m_{NO_x}	The nitrogen oxide emission per unit area, kg/m^2
f_{CO_2}	The emission factor of carbon dioxide, kg/kgce or kg/m^3
f_{SO_2}	The emission factor of sulfur dioxide, kg/kgce or kg/m^3
f_{NO_x}	The emission factor of nitrogen oxide, kg/kgce or kg/m^3
T_{amb}	The ambient temperature, °C

Abbreviation

GSHP	Groud-source heat pump
ASHP	Air-source heat pump
WGB	Wall hanging gas boiler
CFB	Coal-fired boiler
DEH	Direct electric heating
ASHPLTES	ASHP combined with latent thermal energy storage
AWHP	Low ambient temperature air-to-water heat pump
AAHP	Low ambient temperature air-to-air heat pump
BPH	Biomass pellet heating
HSCW	Hot summer and cold winter

broad application of air thermal energy for space heating systems (Aste et al., 2020). As a clean and energy-efficient heat source, ASHP converts low-grade air thermal energy into high-grade energy and saves fossil fuel consumption such as coal and natural gas (Shao et al., 2021).

The ASHP has been increasingly used in recent years because of energy efficiency, environmental friendliness, and stable operation performance (Zhang et al., 2020). Improving the performance of ASHP has become one of the research interests for energy efficiency and indoor thermal environment improvement (Dong et al., 2018). Some research results showed that the COP of ASHP was higher than 3.0 when the ambient temperature was significantly low (Xu et al., 2020). Cooperation with radiant floor heating systems can further reduce the water supply temperature of the heating system and significantly improve the performance of ASHP (Ala et al., 2019; Cheon et al., 2019). Soroush Rastegarpour et al. (Rastegarpour et al., 2020) proposed a linear time-varying model predictive control (MPC) strategy for the ASHP coupled radiant floor heating system, which was proved to save 6 % energy consumption and improve the indoor thermal comfort by 4 % compared to the standard MPC. The experimental research results conducted by Yaning Zhang et al. (Zhang et al., 2017a) showed that the higher zone air temperature and lower ambient temperature resulted in lower COP of ASHP of 1.04– 2.44. Pin Wu et al. (Wu et al., 2020) found that the combination of ASHP and water storage tank could increase the COP of ASHP by 14 %. Huan Zhang et al. (Zhang et al., 2019) developed a novel thermal storage radiator coupled with an ASHP heating system, which could maintain a comfortable indoor environment during the defrosting procedure.

ASHP should be primarily applied for space heating in China's HSCW zones for energy efficiency and carbon neutrality. Firstly, the average ambient air temperature in winter ranges from 0 °C to 10 °C in these areas (Xiong et al., 2019), of which the climate characteristics are particularly suitable for applying ASHP to avoid the risk of frosting (Li et al., 2019). Moreover, the carbon neutrality goal applauds the widespread application of renewable energy sources to replace conventional fossil fuel-based combustions. Even the large-scale use of wall-hanging gas boilers (WGB) fueled by natural gas for space heating will also generate greenhouse gases such as carbon dioxide, which is a significant obstacle to achieving carbon neutrality (Guo & Goumba, 2018).

The achievement of the carbon neutrality goal makes it necessary to replace wall-hanging gas boilers with other equipment with clean energy, such as air-source heat pumps. An analysis of the advantages of air-source heat pumps in replacing WGB in terms of energy efficiency, economics, and carbon dioxide emissions is beneficial to developing and implementing relevant policies. However, the space heating system is still dominated by WGB in the HSCW zones of China. The Building Services Research and Information Association (BSRIA) estimated that there were 10 million homes heated by WGB and only 1 million homes heated by ASHP (Long et al., 2021). Currently, the energy and economic savings potential of the application of the ASHP for space heating systems in HSCW zones of China have not been experimentally or numerically studied. The previous research focused on the economic and environmental improvement of ASHP applied for space heating in northern China (Zhang et al., 2017b), where the heat loads for those areas ranged from 20 W/m^2 ~ 30 W/m^2 caused by the specific ambient conditions and thermal properties of envelopes differing mainly from that of the typical residential buildings in HSCW zones in China (Deng et al., 2021). Therefore, a comparative study on the energy-saving and carbon dioxide emission performance of ASHP and WGB is urgent to evaluate the necessity of replacing WGB with ASHP and provide references for relevant policy planning in HSCW zones in China.

In this research, the energy savings and economic potential of ASHP and WGB heating systems are intended to assess their comparative feasibility for application in HSCW zones in China. The heat loads, primary energy consumption, carbon dioxide, sulfur dioxide, and nitrogen oxide emissions, initial investment, and running cost of both heating systems for residential buildings in the typical cities of these areas were comprehensively analyzed and compared. The theoretical mathematical models of the primary energy consumption, emissions, and economic performance were developed for the ASHP and WGB heating systems. The experimental ASHP and WGB integrated with radiant floor heating systems were established, and the developed theoretical models were validated by the experimental results, which can provide a reference for the widespread application of ASHP for space heating systems in HSCW zones in China and are of great significance for energy saving and carbon neutrality.

Methodology

Mathematical model

The mathematical models of primary energy consumption for ASHP and WGB are demonstrated below. The primary energy consumption for the ASHP heating system can be calculated as follows.

$$Q = \beta_{ec} Q_{hl} / COP_{ASHP} / \eta_{gt} / \eta_{ge} \tag{1}$$

$$\beta_{ec} = 1/LHV_{sc} \tag{2}$$

$$COP_{ASHP} = 0.002 * T_{amb}^{2} + 0.0432 * T_{amb} + 2.752 \tag{3}$$

where Q is the power consumption of ASHP, $kgce/m^2$. Q_{hl} is the heat load of the space heating system, kWh/m^2. β_{ec} is the standard coal coefficient of electricity, 0.1229 kgce/kWh (State Administration for Market Regulation, 2020). LHV_{sc} is the lower calorific value of standard coal, 29.3076 MJ/kg (State Administration for Market Regulation, 2020). η_{gt} is the power transmission efficiency, 92 %. η_{ge} is the average power generation efficiency, 35 %. COP_{ASHP} is the coefficient of performance of ASHP that is related to the water supply temperature, ambient temperature, and other performance factors. COP_{ASHP} can be fitting as the ambient temperature curve, and the ambient temperature can be exported from the typical meteorological dataset. Other performance parameters of a typical ASHP are considered the same as the experimental ASHP below.

The primary energy consumption for the WGB heating system can be calculated as follows.

$$Q = \beta_{ec} Q_{hl} / \eta_{ng} \tag{4}$$

where η_{ng} is the heating efficiency of WGB, assumed to be constant at 90 %.

The primary emissions caused by the ASHP and WGB heating systems are CO_2, SO_2, and NO_x which are the primary pollution sources of global warming, haze, and acid rain. The specific calculation methods for these pollution sources are shown below.

$$m_{emission} = \begin{cases} \begin{cases} m_{CO_2} = f_{CO_2} * Q \\ m_{SO_2} = f_{SO_2} * Q \quad \text{for ASHP} \\ m_{NO_x} = f_{NO_x} * Q \end{cases} \\ \begin{cases} m_{CO_2} = f_{CO_2} * Q / LHV_{ng} \\ m_{SO_2} = f_{SO_2} * Q / LHV_{ng} \quad \text{for WGB} \\ m_{NO_x} = f_{NO_x} * Q / LHV_{ng} \end{cases} \end{cases} \tag{5}$$

where f_{CO_2}, f_{SO_2}, and f_{NO_x} are the emission factors of the standard coal which are 2.493 kg/kgce, 0.075 kg/kgce, and 0.0375 kg/kgce, 1.94 kg/m^3, 0.00124 kg/m^3, and 0.00496 kg/m^3 of natural gas (Yu et al., 2021). LHV_{ng} is the lower calorific value of natural gas, 35.59 MJ/m^3 (State Administration for Market Regulation, 2020). m_{CO_2}, m_{SO_2}, m_{NO_x} are the carbon dioxide, sulfur dioxide, and nitrogen oxide emissions per unit area, kg/m^2.

Building heat load

The typical cities including Chongqing, Chengdu, Shanghai, Hangzhou, Wuhan, and Changsha in the HSCW zones of China are shown in Fig. 1. The HSCW zones of China are where the average ambient temperature of the coldest month is between 0– 10 °C, and the average temperature of the hottest month is between 25–30 °C. The average daily temperature below 5°*C* counts for 0– 90 days, and the average daily temperature above 25°*C* counts for 49– 110 days. The selected six cities are the representative cities of the HSCW zones. The heating calculation period should be December 1 of the year to February 28. The typical meteorological dataset based on the monthly average of the last 10 years is used for ambient parameter calculation. The annual ambient temperatures of the six distinctive cities in the HSCW zones of China are shown in Fig. 2.

The designed zone air temperature is set at 18°C, and the ventilation time is 1.0 times/h. The calculated heat loads of the typical residential buildings for the six cities in the HSCW zones of China are shown in Table 1. The configuration specifications of the typical buildings are shown in the experimental sections.

Theoretical techno-economic analysis

The energy consumption, carbon dioxide emission, sulfur dioxide emission, nitrogen oxide emissions, the heating cost, and the running cost of the ASHP and WGB heating systems are calculated according to the developed mathematical models above. The calculation results are analyzed in this section.

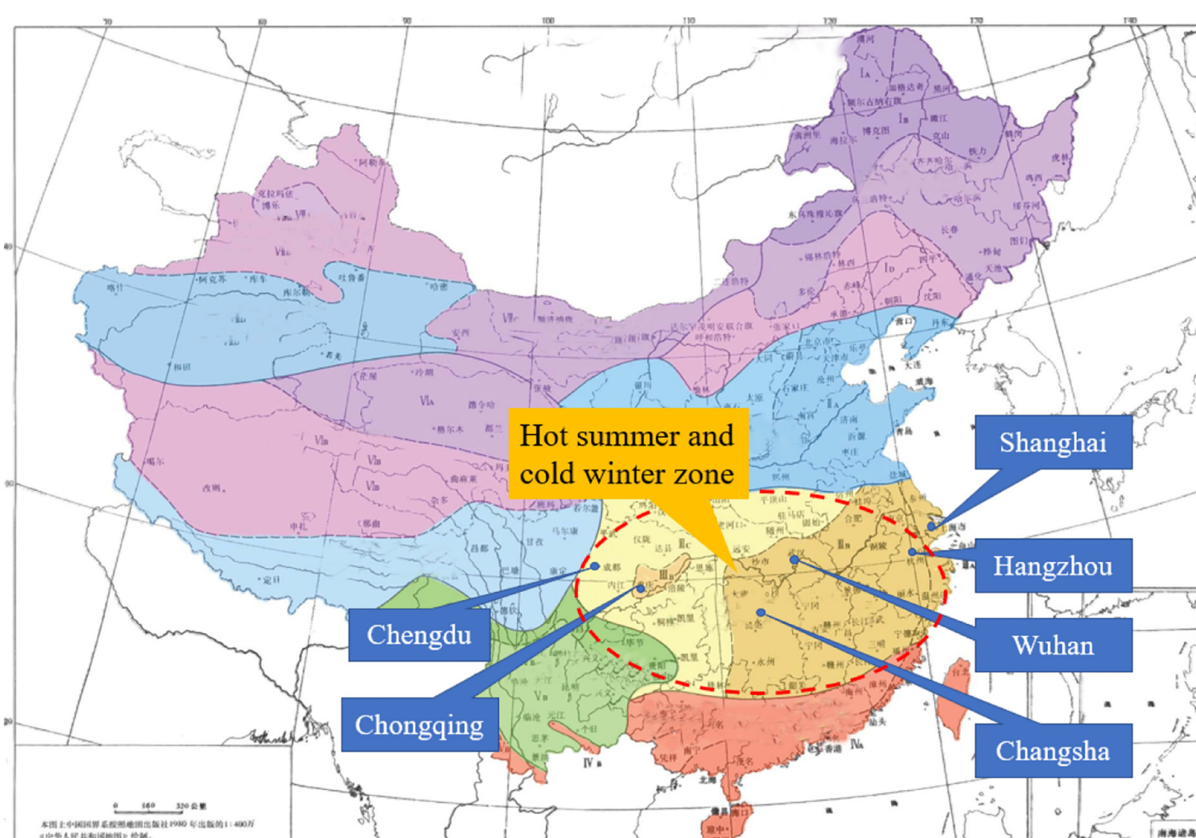

Fig. 1. The six typical cities in the HSCW zones of China.

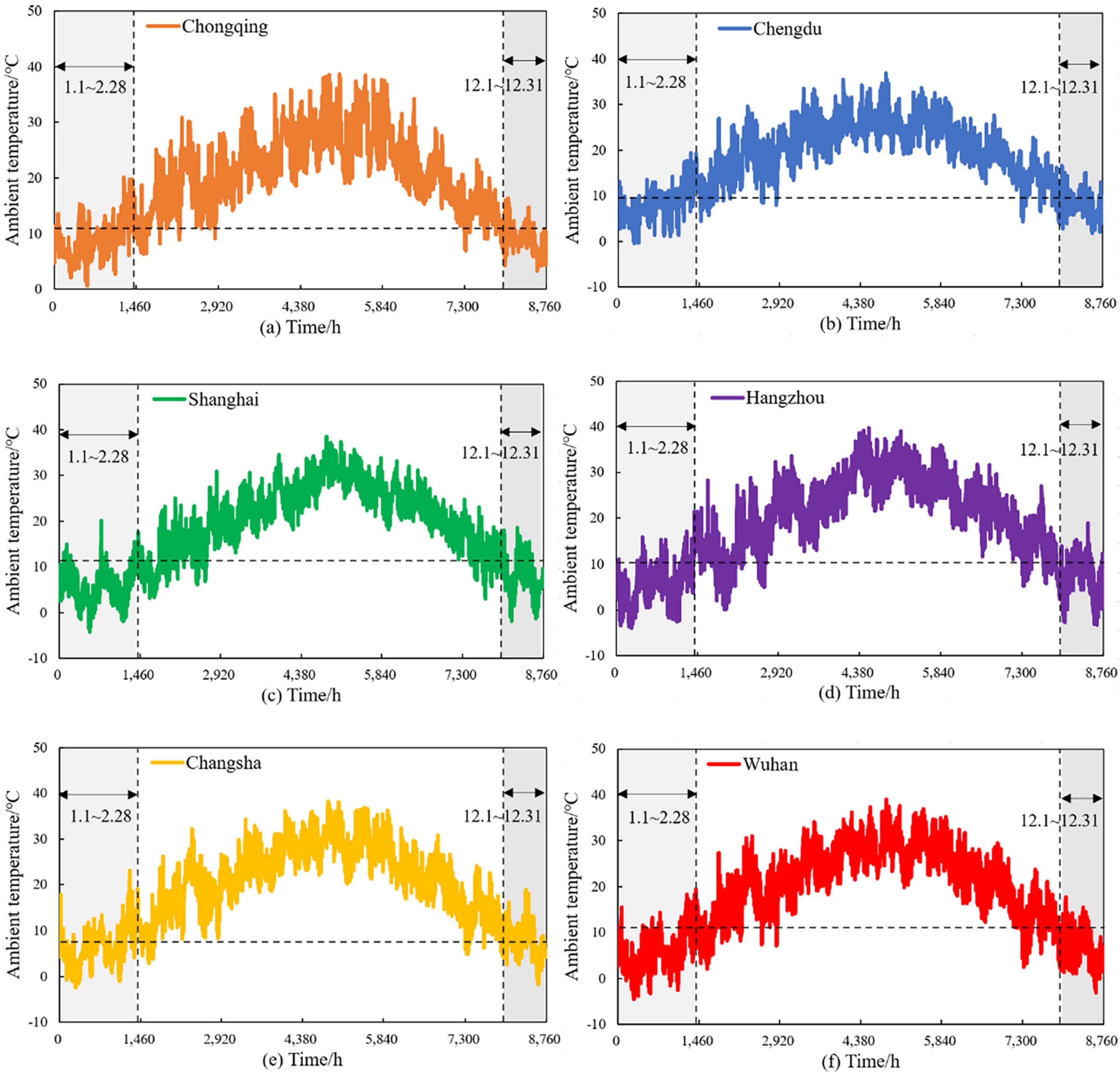

Fig. 2. Annual ambient temperatures of the six typical cities in the HSCW zones of China (China Meteorological Administration Meteorological Data Center, 2022).

Primary energy consumption analysis

The primary energy consumption per unit area of the ASHP and WGB heating systems for residential buildings in the six cities of HSCW zones in China is shown in Fig. 3. The primary energy consumption is close for both ASHP and WGB heating systems in different cities. The average primary energy consumptions of the ASHP and WGB heating systems are 10.97 kgce/m^2 and 12.5 kgce/m^2, respectively. The WGB heating system consumes 12.3 % more primary energy consumption than the ASHP heating system. The primary energy consumption, emissions, heating cost, and

Table 1
The calculated heat loads of the typical residential buildings for the six cities in the HSCW zones of China.

Item	Chongqing	Chengdu	Shanghai	Hangzhou	Changsha	Wuhan
Designed zone air temperature (°C)	18	18	18	18	18	18
Ambient air temperature (°C)	Typical meteorological dataset					
Calculated COP of ASHP	3.30	3.23	3.16	3.13	3.19	3.11
The heat load of the typical building 1 (W/m^2)	40.77	42.12	43.89	44.90	43.26	45.63
The heat load of the typical building 2 (W/m^2)	40.21	40.56	40.52	42.04	41.37	43.11
Average heat load (W/m^2)	40.49	41.34	42.20	43.47	42.32	44.37
Heat consumption (kWh/m^2)	87.46	89.29	91.16	93.88	91.40	95.83

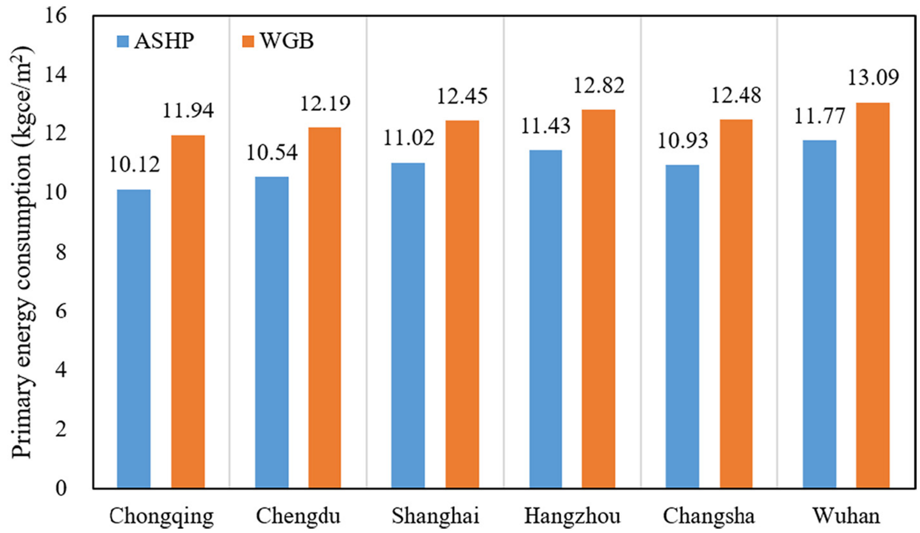

Fig. 3. The primary energy consumption of the ASHP and WGB heating systems.

running cost of the ASHP and WGB heating systems of the typical six cities in HSCW zones of China are shown in Table 2.

Carbon dioxide emission analysis

The carbon dioxide emissions per unit area of the ASHP and WGB heating systems for residential buildings in the six cities of HSCW zones in China are shown in Fig. 4. The carbon dioxide emission of the ASHP heating systems ranges from 25.22 kg/m^2 ~ 29.34 kg/m^2, while that of the WGB heating system ranges from 19.08 kg/m^2 ~ 20.91 kg/m^2. The average carbon dioxide emissions of the ASHP and WGB heating systems are 27.35 kg/m^2 and 19.96 kg/m^2, respectively. The ASHP heating system causes 36.9 % more carbon dioxide emissions than the WGB heating system.

Sulfur dioxide and nitrogen oxide emissions analysis

The sulfur dioxide and nitrogen oxide emissions per unit area of the ASHP and WGB heating systems for residential buildings in the six cities of HSCW zones in China are shown in Fig. 5. The total sulfur dioxide and nitrogen oxide emissions of the ASHP heating system are far more than that of the WGB heating system, which are 1.23 kg/m^2 and 0.06 kg/m^2 on average, respectively. The average sulfur dioxide and nitrogen oxide emissions of the ASHP and WGB heating systems are 27.35 kg/m^2 and 19.96 kg/m^2, respectively. The ASHP heating system leads to 19.3 times of total sulfur dioxide and nitrogen oxide emissions than the WGB heating system.

Economic analysis

According to the previous research results on the different heating sources integrated with radiant floor heating systems, the total initial costs for the ASHP and WGB integrated with radiant floor heating systems are 240 CNY /m^2 and 180 CNY /m^2 including other infrastructures such as water splitter and mixer (Zhang et al., 2017b). For the running cost calculation, the unit prices of standard coal, natural gas, and electricity are 880 CNY/ton, 2.05 CNY/m^{3}And 0.50 CNY/kWh (Deng et al., 2021), respectively. The maintenance costs of the ASHP and WGB heating systems are 1 % of their initial investments. The running costs, including the heating and maintenance costs of the ASHP and WGB

Table 2
The primary energy consumption, emissions, heating cost, and running cost of the ASHP and WGB heating systems of the typical six cities in HSCW zones of China.

Item	System	Chongqing	Chengdu	Shanghai	Hangzhou	Changsha	Wuhan	Average
Q	ASHP	10.12	10.54	11.02	11.43	10.93	11.77	10.97
(kgce/m^2)	WGB	11.94	12.19	12.45	12.82	12.48	13.09	12.50
Relative ratio (%)		−15.3 %	−13.6 %	−11.5 %	−10.8 %	−12.4 %	−10.1 %	−12.3 %
CO_2	ASHP	25.22	26.28	27.48	28.50	27.26	29.34	27.35
(kg/m^2)	WGB	19.08	19.48	19.89	20.48	19.94	20.91	19.96
Relative ratio (%)		32.2 %	34.9 %	38.2 %	39.1 %	36.7 %	40.4 %	36.9 %
SO_2	ASHP	0.76	0.79	0.83	0.86	0.82	0.88	/
(kg/ m^2)	WGB	0.01	0.01	0.01	0.01	0.01	0.01	
NO_x	ASHP	0.38	0.40	0.41	0.43	0.41	0.44	
(kg/m^2)	WGB	0.05	0.05	0.05	0.05	0.05	0.05	
SO_2+NO_x	ASHP	1.14	1.19	1.24	1.29	1.23	1.32	1.23
	WGB	0.06	0.06	0.06	0.07	0.06	0.07	0.06
Multiple		18.7	19.0	19.5	19.6	19.3	19.8	19.3
Heating cost	ASHP	14.41	15.01	15.69	16.28	15.57	16.76	15.62
(CNY/m^2)	WGB	20.16	20.58	21.01	21.64	21.07	22.09	21.09
Relative ratio (%)		−28.5 %	−27.1 %	−25.3 %	−24.8 %	−26.1 %	−24.1 %	−26.0 %
Maintenance cost	ASHP	2.40	2.40	2.40	2.40	2.40	2.40	2.40
(CNY/m^2)	WGB	1.80	1.80	1.80	1.80	1.80	1.80	1.80
Total operation cost	ASHP	16.81	17.41	18.09	18.68	17.97	19.16	18.02
(CNY/m^2)	WGB	21.96	22.38	22.81	23.44	22.87	23.89	22.89
Relative ratio (%)		−23.5 %	−22.2 %	−20.7 %	−20.3 %	−21.4 %	−19.8 %	−21.3 %

Note: Relative ratios of the heat loads, emissions, heating costs, and maintenance costs are defined as *Relative ratio* $(\%) = \frac{Q_{ASHP} - Q_{WGB}}{Q_{WGB}}$.

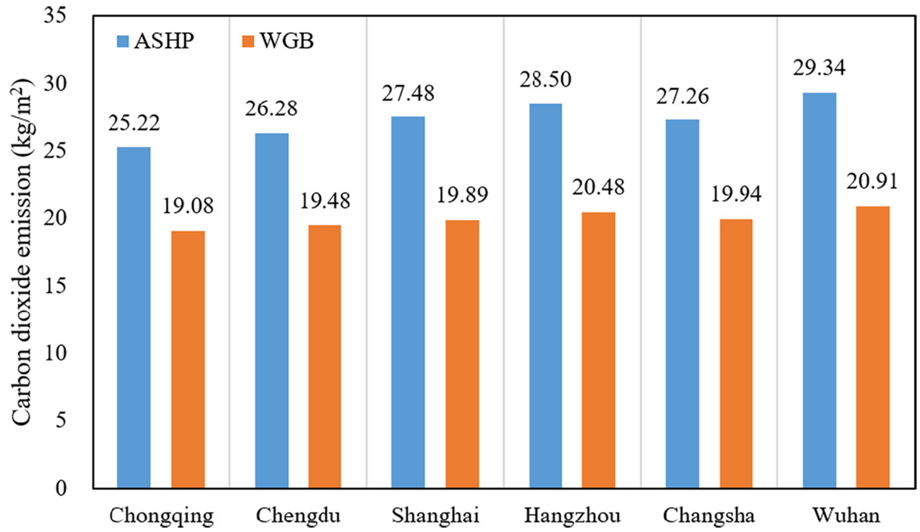

Fig. 4. The carbon dioxide emissions of the ASHP and WGB heating systems.

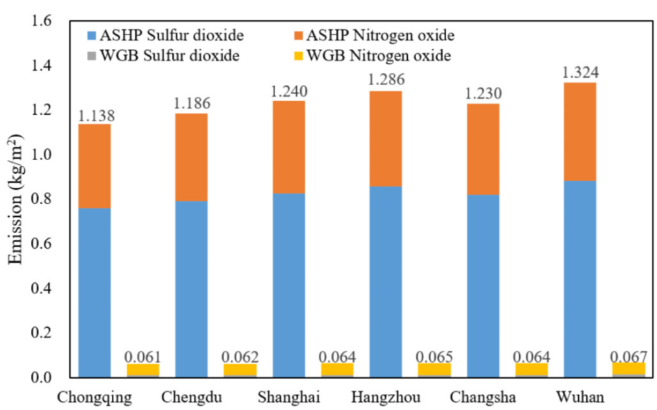

Fig. 5. The sulfur dioxide and nitrogen oxide emissions of the ASHP and WGB heating systems.

heating systems, are shown in Fig. 6. The heating costs of the ASHP and WGB heating systems are 15.62 CNY/m^2 and 21.09 CNY/m^2 on average, respectively, the heating cost of the ASHP system is 26.0 % less than that of the WGB system. The total running costs of the ASHP and WGB heating systems are 18.02 CNY/m^2 and 22.89 CNY/m^2 and the ASHP heating system can save 21.3 % of running cost than that of the WGB heating system.

The running cost calculation is based on the calculated average coefficient of performance of ASHP according to the ambient temperatures of the typical meteorological dataset. The sensitivity analysis showed that a 20 % reduction in COP could result in a 28 % increase in the primary energy consumption and a 20 % running cost increase for the ASHP heating system (Zhang et al., 2017b).

Experimental measurements of both heating systems

Two sets of experimental cells of radiant floor heating systems were established with the ASHP and WGB for both heating systems' energy-saving potential and economic benefits comparisons.

The air-source heat pump system

The schematic diagram of the experimental cells for the ASHP and WGB heating systems is shown in Fig. 7. The experimental cell for the

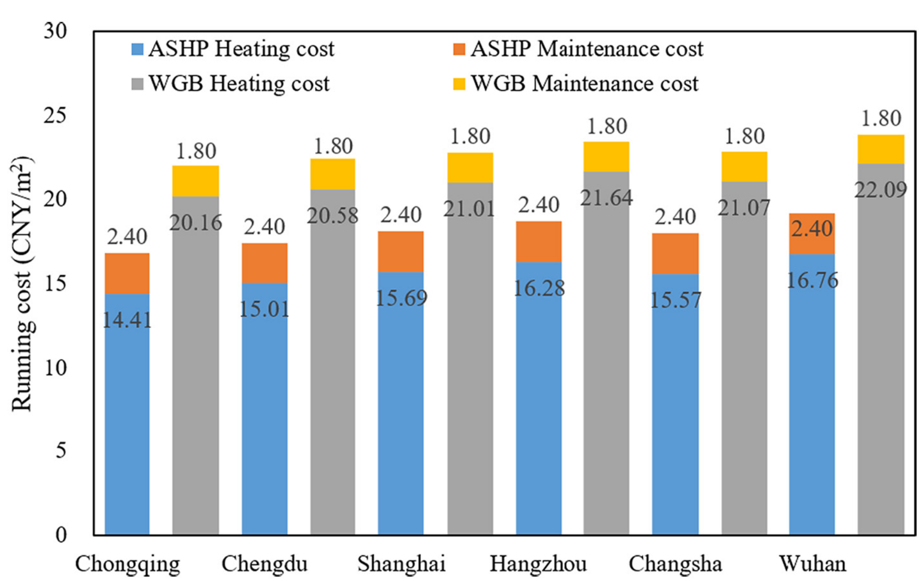

Fig. 6. The running costs including of the heating and maintenance costs of the ASHP and WGB heating systems.

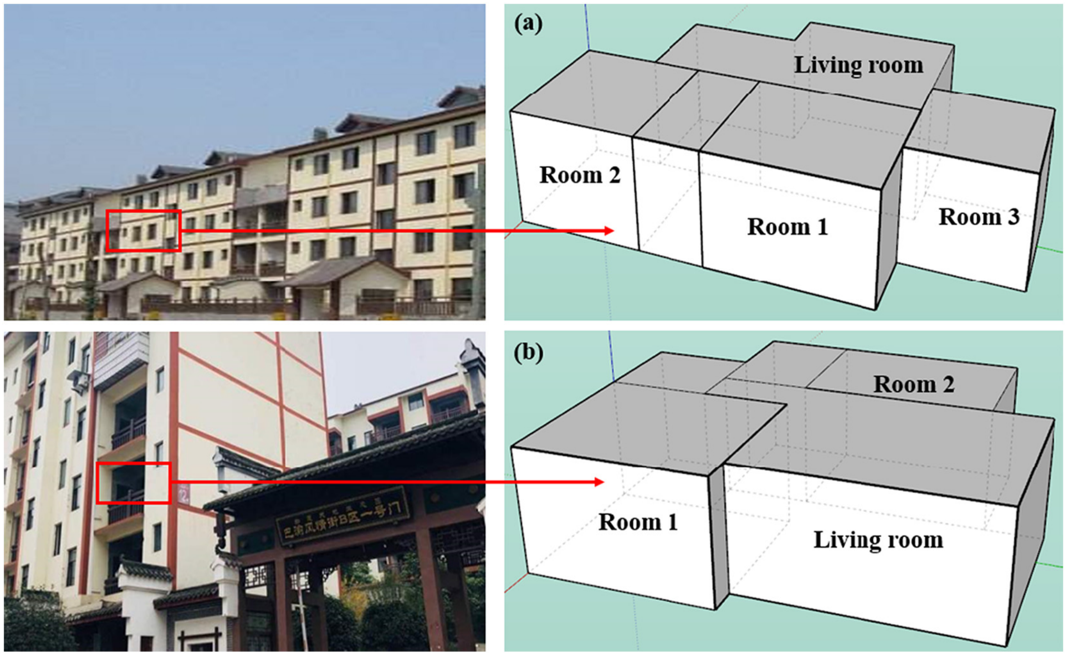

Fig. 7. Schematic diagram of the experimental cells for (a) the ASHP heating system and (b) the WGB heating system.

ASHP heating system consists of three bedrooms and a large living room with infrastructure such as bathrooms, kitchens, balconies, etc. The dimensions of the three bedrooms and the living room are 4.2 m * 3.6 m, 3.3 m * 3.6 m, 3.0 m * 3.0 m, and 7.2 m * 3.9 m, respectively, with a floor height of 2.7 m. The integrated capillary-mat radiant floor applied in this research has a pipe spacing of 2 cm and a size of 1000 mm * 2500 mm, which is highly integrated and easily installed compared to the ordinary radiant floor systems. There are no installed radiant floors in bathrooms and kitchens in residential buildings since these areas are not occupied for long periods. The total area of system 1 is 60.18 m^2 of which 48.60 m^2 of the floor area is covered with capillary mats, accounting for approximately 81 % of the total floor areas. The specific configuration and thermal performance of the building envelopes and windows are shown in Table 3. The ASHP heating system adopts a variable-speed air-source heat pump, model DTAWR-100 V/C, with a rated heating capacity of 11 kW and a rated heating power of 3.2 kW in heating mode. The air-source heat pump is placed on an open deck outside bedroom 1, fully exposed to the ambient environment for adequate heat exchange between the air-source heat pump and the outdoor air.

Table 3
The specific configuration and thermal property of the building envelopes and windows.

Envelopes	Material	Heat transfer coefficient ($W/m^2 \cdot K$)	Thermal resistance($m^2 \cdot K/W$)
Exterior Walls	Cement mortar 20 mm Inorganic insulation mortar 30 mm Sintered shale porous brick masonry 240 mm Cement mortar 20 mm	1.10	0.91
Partition walls	Cement mortar 20 mm Sintered shale porous brick masonry 240 mm Cement mortar 20 mm	1.46	0.69
Floor	Ceramics 10 mm Active layer for heating Concrete backfills 50 mm XPS 20 mm Cement mortar 20 mm Reinforced concrete 120 mm Cement mortar 20 mm	0.99	1.01
Door	Wooden doors	2.47	0.40
Exterior Windows	Plastic window frames (25 % of window frame area) 6 + 9A + 6 double glazing	2.50	0.40

The wall-hanging gas boiler system

The schematic diagram of the experimental cells for the WGB heating system is shown in Fig. 7 (b). Due to the limited space of the experimental cells, there was no way to install the air-source heat pump and the wall-hanging gas boiler in the same radiant floor heating system. Therefore, the WGB heating system was installed in another similar apartment in the same community. The experimental cells for system 2 consist of a bedroom, a study, and a large living room and include infrastructure such as bathrooms, kitchens, balconies, etc. The bedroom, study, and living room dimensions are 3.3 m * 3.9 m, 3.9 m * 1.8 m, and 3.3 m * 4.5 m, respectively, with a floor height of 3 m. The radiant floors are covered with the same dimensional capillary mat as system 1, of which the specification has been illustrated in the above context. The total area of system 2 is 37.44 m^2 of which 30.50 m^2 of the floor area is covered with capillary mats, accounting for approximately 81 % of the total floor areas, with no capillary mat covered in areas such as bathrooms and kitchens like the ASHP heating system.

The WGB heating system adopts a wall-hanging gas boiler, model L1PB20-HT1(T), which has a rated heating capacity of 7.9 kW ~ 20 kW, rated heating power of 125 W, and a maximum water supply temperature of 90 °C. The construction drawing of the experiment sites for the ASHP and WGB integrated with radiant floor heating systems is shown in Fig. 8.

Experimental measurements

Details of the experimental cell setups of both radiant floor heating systems with ASHP and WGB as heat sources are presented, and the heat loads of both radiant floor heating systems were very close. First, the heat loads of the building envelopes of the two experimental cells were relatively close due to the more considerable floor height of the WGB system with the rather more minor radiant floor area. Secondly, there was a floor-to-ceiling window in both bedrooms and the large

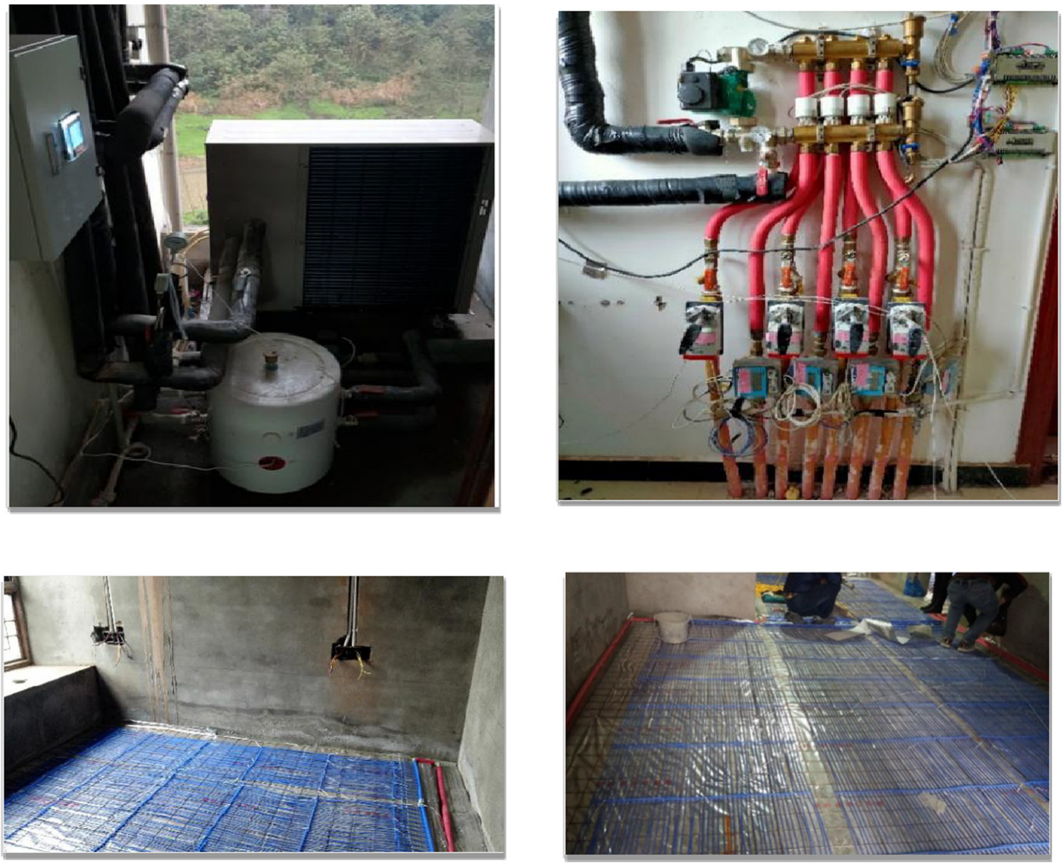

Fig. 8. Construction drawing of the experiment sites for the ASHP and WGB integrated with radiant floor heating systems.

living room of the WGB system, which significantly increased the heat load of the transparent enclosures. Moreover, the boundary conditions of the building envelope were different for the two systems. The boundary temperature of the building envelopes was higher for the ASHP system because the neighbouring zones were heated. However, the boundary temperature of the building envelopes was lower for the WGB system because there were no occupants in the adjacent zones, which reasonably explained the closer heat load of the two systems. The heat load per unit area of the experimental cells for the ASHP and WGB heating systems is shown in Table 4, while the calculated ambient temperature was 10°C. The relative rates of −3.08 % ~ 1.56 % under the zone air temperature of 22°C, 20°C, and 18°C can prove the nearly identical heat load and the proper experimental cells setup for the ASHP and WGB heating systems.

In this research, the energy consumption and the running cost of the ASHP and WGB heating systems were calculated and analyzed through the experimental measurements of the heat supply, the electricity consumption, the natural gas consumption, the electricity charges, and natural gas charges. During the experiment, the following parameters were measured and recorded at 5-min intervals: internal surface temperatures of the building envelopes and zone air temperatures by T-type thermocouples, ambient parameters such as the ambient temperature, the relative humidity, and solar radiation by the meteorological observation station, the heat supply of each thermal zone of the two systems by the heat meter, the electricity consumption of the ASHP by the electricity meter, natural gas consumption of the WGB by the natural gas flow meter. The surface temperatures are measured in a five-point arrangement equally divided along the diagonal, shown in Fig. 9. The relative experimental error of zone air and surface temperatures is 2.7 %. The relative error of heat supply is 1.8 %, and the relative error of electricity and natural gas consumption is 1.0 %. The relative errors in primary energy consumption and emissions for the ASHP and WGB systems are 3.4 % and 1.8 % since the performance of the ASHP was related to COP. In contrast, the performance of the WGB was consumed as a constant. The relative error of the running cost of both is 1 % based on the measurement error of the equipment.

Table 4
The experimental cells' heat load per unit area for the ASHP and WGB heating systems.

Heat load (W/m^2)	22°C	20°C	18°C
The ASHP system	61.94	51.05	38.91
The WGB system	60.09	49.81	39.53
Relative rate	−3.08 %	−2.49 %	1.56 %

Experimental results and discussion

To evaluate the energy consumption, emission, and economic performance of the ASHP and WGB systems for space heating in HSCW zones in China, the experimental tests in Chongqing as one of the typical cities were conducted from December 28 to January 18.

The two heating systems were in operation under the same ambient conditions. The daily average ambient temperature ranged from 5.1°C to 10.4°C during the experimental period. The average zone air temperatures of the ASHP and WGB heating systems were 18.53°C and 18.45°C, as shown in Fig. 10, close to 18°C of the designed zone air temperature for space heating systems in HSCW zones of China.

The average heat loads of the ASHP and WGB heating systems are shown in Fig. 11. The average heat loads of the ASHP and WGB heating systems were 45.73 W/m^2 and 42.98 W/m^2 during the experimental period, both average heat loads were close and slightly lower than the calculated value of the whole heating season, for which the experimental period's relatively lower average ambient temperature should be responsible. Overall, the measured heat loads of both heating systems

Fig. 9. Arrangement of temperature measurement points.

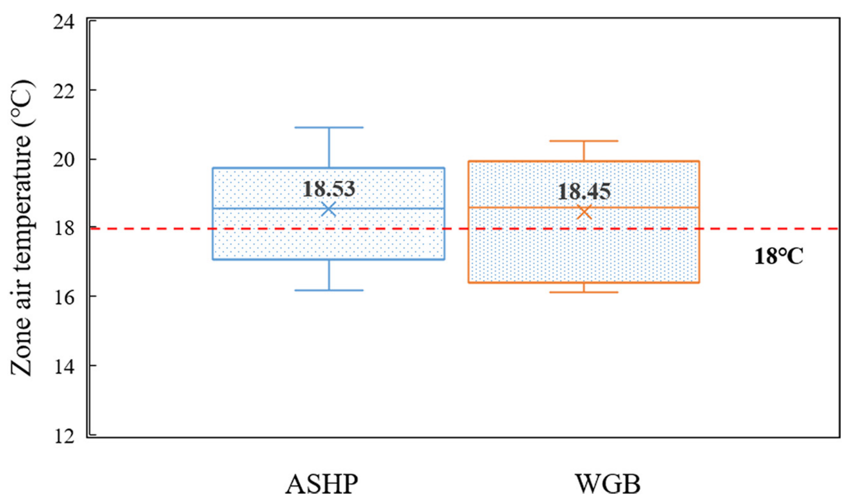

Fig. 10. The average zone air temperatures of the ASHP and WGB heating systems.

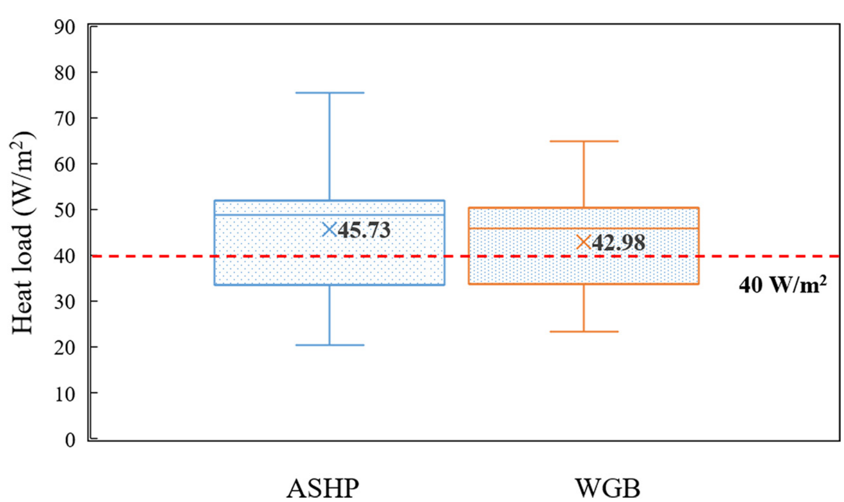

Fig. 11. The average heat loads of the ASHP and WGB heating systems.

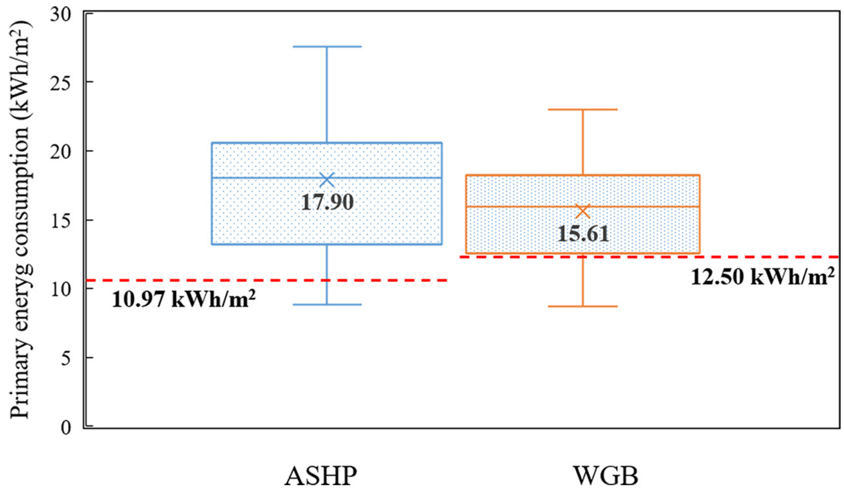

Fig. 12. The primary energy consumption of the ASHP and WGB heating systems.

for typical residential buildings in Chongqing were fundamentally consistent with the simulation results.

Energy consumption analysis

The primary energy consumptions of the ASHP and WGB heating systems are shown in Fig. 12. The primary energy consumption of the whole heating season was estimated according to the experimentally average electricity and natural gas consumptions of the ASHP and WGB heating systems for more precise comparison of the mathematical model analysis and the experimental results. The experimental primary energy consumption of the ASHP system was 17.90 kWh/m^{2}for the whole heating season, which was 39 % higher than the theoretical analysis result of 10.97 kWh/m^2. This is due to the COP of ASHP with an average of 1.92, which was 42 % lower than the calculated COP of 3.30. This discrepancy between the theoretical and experimental primary energy consumptions caused by the discounted COP was expected according to the sensitivity analysis of primary energy consumption and running cost with COP (Zhang et al., 2017b).

Besides, the calculated experimental primary energy consumption of the WGB system was 15.61 kWh/m^2, which was 30 % higher than the theoretical analysis result of 12.50 kWh/m^2. The slightly higher experimental heat load of the residential buildings and the average 73 % of the heating efficiency of the WGB system caused by the heat loss of the water distribution systems and other equipment were the main reason for the discrepancy between the theoretical and experimental primary energy consumption of the WGB heating system. Besides, the distributed space heating system was dominated in this area, which meant that adjacent zone temperature difference and thermal insulation of radiant floor were also responsible for this phenomenon. Therefore, passive insulation technology development is also a research interest that needs to be intensively studied in HSCW zones.

Heating cost analysis

The heating costs of the ASHP and WGB heating systems are shown in Fig. 13. Similarly, the heating costs of the whole heating season were approximated according to the calculated average values of the experimentally measured electricity and natural gas consumption of the ASHP and WGB heating systems. The calculated experimental heating cost of the ASHP system was 25.49 CNY/m^2, which was 39 % higher than the theoretical analysis result of 15.62 kWh/m^2. The reduced COP of ASHP caused this in the experimental period. The calculated experimental heating cost of the WGB system was 26.36 CNY/m^2, which was 20 % higher than the theoretical analysis result of 21.09 kWh/m^2. This can be reasonably explained by the lower heating efficiency of the WGB system compared with the theoretical situation.

Carbon dioxide emission analysis

The carbon dioxide emissions of the ASHP and WGB heating systems are shown in Fig. 14. Similarly, the carbon dioxide emissions of the

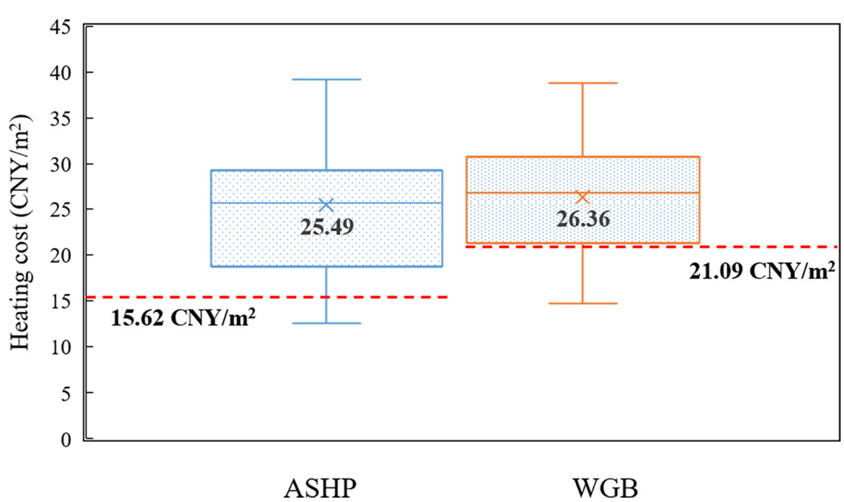

Fig. 13. The heating costs of the ASHP and WGB heating systems.

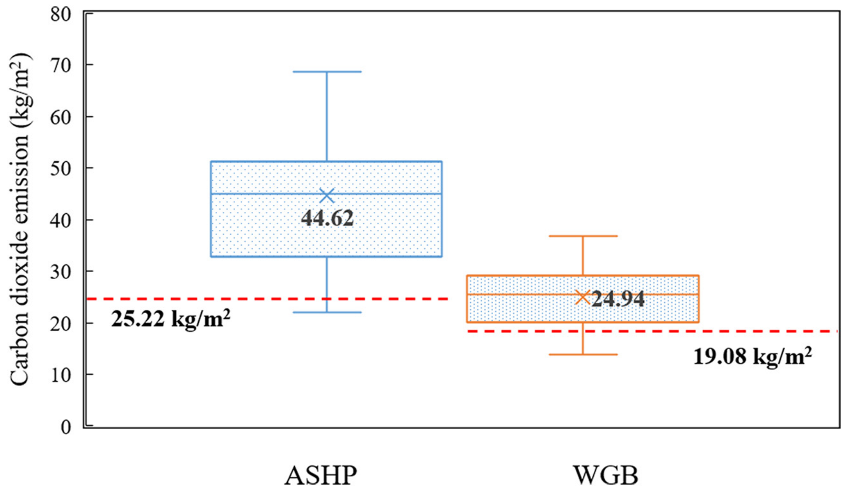

Fig. 14. The carbon dioxide emissions of the ASHP and WGB heating systems.

whole heating season were calculated on average according to the experimental results. The sulfur dioxide and nitrogen oxide emissions were too small and excluded from the calculation and analysis. The calculated experimental carbon dioxide emission of the ASHP system was 44.62 kg/m^2, which was 43 % higher than the theoretical analysis result of 25.22 kg/m^2. The calculated experimental carbon dioxide emission of the WGB system was 24.94 kg/m^2, which was 24 % higher than the theoretical analysis result of 19.08 kg/m^2. The reduced COP of ASHP enlarged the discrepancy of the carbon dioxide emissions between the ASHP and WGB heating systems. The calculated experimental heat consumption, primary energy consumption, heating cost, and carbon dioxide emission of the ASHP and WGB heating systems are shown in the appendix. The experimental values averaged the normalized value of the heating period since the experimental measurement did not cover the whole heating period.

Discussion

Previous research comparisons of energy consumption, environmental impact, and economic performance of space heating systems under different heat source forms and different climate zones are shown in Table 5. Dong et al. (2021) evaluated the thermal comfort, energy consumption, pollutant emissions, and economic performance of different heat sources of CFB, WGB, DEH, ASHP, electric heating film, and solar heating. Only the research results of the ASHP and WGB heating systems were compared with that of other literature studies

Table 5
Previous research comparisons of energy consumption, environmental impact, and economic performance of heating systems under different heat source forms and different climate zones.

Areas	Evaluation metrics	Heat load (W/m^2)	Zone (m^2)	Heat sources	Heat terminals	Comparison	Q (kgce/m^2)	Emissions (kg/m^2)		Operation cost (CYN/m^2)	COP
								CO2	SO2 & NOX		
Dong et al. (2021)											
Rural areas in Lanzhou	Thermal comfort Energy Environment Economy	35– 45	120	CFB WGB DEH ASHP Electric heating film Solar heating	Fin radiator Floor radiation Fan coil	ASHP WGB Ratio	23.1 34.7 −33.5 %	35.4 59.5 −40.5 %	0.6 0.6 0.99	19.6 27.1 −27.9 %	1.69–1.75
Zhang et al. (2017b)											
Northern China / Beijing	Energy Environment Economy	20.5	808.71	CFB ASHP LargeCFB RegionalCFB WGB DEH	/	ASHP WGB Ratio	7.4 8.1 −8.6 %	18.3 11.7 56.4 %	0.828 0.039 21.23	13.2 13.2 0.0 %	3.1
Deng et al. (2021)											
Northern rural China / Beijing	Energy Environment Economy	Typical rural houses		RawCFB ShapedCFB BPH AWHP AAHP	Radiator	AWHP AAHP Ratio	41.2 (kWh/m^2) 16.9 (kWh/m^2) 59.0 %	33.8 13.9 59.0 %	0.0308 0.0127 2.43	20.6 8.5 58.7 %	/
Yu et al. (2021)											
Beijing Shanghai Shenyang Harbin	Energy Environment Economy	30– 67	100	CFB WGB DEH ASHP ASHPLTES	/	ASHP WGB ASHPLTES Ratio	4.99–26.45 6.51–21.21 5.49–25.22 −23.3 %	40.5–214.56 10.4–34.98 44.56 ~204.63 74.3 %	1.83 ~9.69 0.04 ~0.11 2.01 ~9.24 45.7	30.34 ~147.87 12.3 ~39.49 33.69 ~141.76 59.4 %	1.82–3.42
This research											
HSCW zones of China	Energy Environment Economy	40– 45	60– 80	ASHP & WGB	Radiant floor heating	ASHP WGB Ratio	10.97 12.50 −12.3 %	27.35 19.96 36.9 %	1.23 0.06 0.1	15.62 21.09 −26.0 %	3.11–3.30

here. The ASHP heating system saved 33.5 % standard coal compared with the WGB system, while the carbon dioxide emission of the former was 40.5 % lower than that of the latter. The ASHP system saved 27.9 % of the operation cost than that of the WGB system when the COP of ASHP was considered as 1.69– 1.75 in the cold areas of China. Zhang et al. (2017b) analyzed the energy consumption, environmental influence, and economic performance of CFB, ASHP, Large CFB, Regional CFB, WGB, and DEH in northern China and took Beijing as an example. The standard coal consumption and operation costs were comparative for both heating systems, while the carbon dioxide emission of the ASHP system was higher than that of the WGB system. The energy consumption was obviously higher than that in Zhang Dong et al.'s research (Dong et al., 2021), caused by the more significant COP of ASHP influenced by the higher ambient temperature in Beijing than in Lanzhou. Deng et al. (2021) compared the space heating systems with heat sources of CFB, BPH, AWHP, and AAHP in northern rural China. The AAHP heating system saved about 59 % of electricity, carbon dioxide emissions, and operation costs more than the AWHP system, which meant the former heat pump was a better alternative in the research areas.

Unlike the above studies that were limited to urban or rural residential buildings in northern or cold zones, Yu et al. (2021) conducted comprehensive research on the different heat sources in representative cities of severe cold, cold, and HSCW zones of China. They developed an ASHP combined with latent thermal energy storage applied for space heating and compared it with CFB, WGB, DEH, and ASHP. The developed ASHPLTES had comparable performance to the normal ASHP in terms of energy, environmental, and economic aspects. In summary, the energy-saving of the ASHP system over the WGB system depended on the climate characteristics. The lower COP limited the outstanding performance of ASHP in the cold northern areas, but this was one of the research interests for the widespread application of ASHP in cold regions in the future. In this research, ASHP saved 23.3 % of standard coal compared with WGB in HSCW zones, demonstrating that ASHP had promising application prospects in these areas.

Conclusion

This study is intended to evaluate the energy savings and economic benefits of the ASHP and WGB heating systems to compare their application feasibility in the HSCW zones of China. A comprehensive analysis of building heat loads, primary energy consumption, carbon dioxide, sulfur dioxide, and nitrogen oxide emissions, initial investment, and operating costs was conducted for residential buildings in typical cities in this area. Theoretical mathematical models of energy consumption, emission, and economic performance of the ASHP and WGB heating systems were developed. The theoretical model calculations demonstrated the 12.3 % saving in primary energy consumption, 36.9 % increase in carbon dioxide emission, and the ASHP heating systems can obtain a 26.0 % reduction in heating cost compared with the WGB system, of which the increased carbon dioxide emission mainly came from the limited power generation and transmission efficiency. The experimental results showed that the discounted COP of ASHP led to a significant decrease in energy savings and economic benefits of the ASHP system compared to the WGB system, which meant that more giant COP enabled the large-scale application of ASHP in HSCW zones in China. The cost of carbon emissions should be factored into the overall operating cost of the heating system in future research. This research can provide a reference for related policy planning for clean space heating and urgent research interests under the carbon neutrality background.

Declaration of competing interest

We declare that we have no financial and personal relationships with other people or organizations that can inappropriately influence our work, there is no professional or other personal interest of any nature or kind in any product, service and/or company that could be construed as influencing the position presented in, or the review of, the manuscript entitled.

Appendix A

The calculated experimental heat consumption, primary energy consumption, heating cost, and carbon dioxide emission of the ASHP and WGB heating systems.

Date	ASHP				WGB			
	Heat consumption W/m^2	Primary energy consumption $kgce/m^2$	Heating cost CNY/m^2	CO_2 kg/m^2	Heat consumption W/m^2	Primary energy consumption $kgce/m^2$	Heating cost CNY/m^2	CO_2 kg/m^2
28-Dec	28.19	0.04	0.18	0.11	33.08	0.14	0.23	0.22
29-Dec	33.54	0.05	0.21	0.13	35.44	0.15	0.24	0.23
30-Dec	42.24	0.07	0.28	0.17	46.10	0.20	0.34	0.32
31-Dec	83.87	0.13	0.51	0.31	64.98	0.26	0.43	0.41
1-Jan	51.92	0.09	0.36	0.22	51.38	0.23	0.39	0.37
2-Jan	48.26	0.07	0.29	0.18	50.92	0.20	0.34	0.32
3-Jan	50.66	0.08	0.31	0.19	51.41	0.21	0.35	0.33
4-Jan	49.25	0.07	0.30	0.19	47.00	0.19	0.32	0.30
5-Jan	49.94	0.07	0.29	0.17	45.64	0.17	0.28	0.27
6-Jan	75.57	0.11	0.44	0.27	64.93	0.24	0.41	0.39
7-Jan	42.03	0.07	0.27	0.16	42.79	0.17	0.29	0.28
8-Jan	54.57	0.08	0.34	0.21	49.10	0.20	0.34	0.33
9-Jan	50.67	0.07	0.30	0.18	46.31	0.18	0.31	0.29
10-Jan	59.06	0.09	0.36	0.22	52.34	0.21	0.35	0.33
11-Jan	54.14	0.08	0.32	0.20	45.90	0.17	0.29	0.28
12-Jan	51.85	0.08	0.33	0.20	49.13	0.20	0.34	0.32
13-Jan	46.44	0.07	0.27	0.17	45.01	0.17	0.29	0.28
14-Jan	33.77	0.05	0.21	0.13	25.40	0.10	0.17	0.17
15-Jan	20.44	0.03	0.14	0.09	23.38	0.10	0.17	0.17
16-Jan	26.92	0.05	0.19	0.12	27.39	0.12	0.21	0.20
17-Jan	24.57	0.04	0.16	0.10	23.80	0.10	0.17	0.17
18-Jan	28.07	0.04	0.17	0.11	24.17	0.10	0.16	0.15
Normalized value of heating period	45.73	17.90	25.49	44.62	42.98	15.61	26.36	24.94

References

Ahn, B. -C., & Song, J. -Y. (2010). Control characteristics and heating performance analysis of automatic thermostatic valves for radiant slab heating system in residential apartments. *Energy*, *35*(4), 1615–1624.

Ala, G., Orioli, A., & Di Gangi, A. (2019). Energy and economic analysis of air-to-air heat pumps as an alternative to domestic gas boiler heating systems in the South of Italy. *Energy*, *173*, 59–74.

Aste, N., Caputo, P., Del Pero, C., et al. (2020). A renewable energy scenario for a new low carbon settlement in northern Italy: Biomass district heating coupled with heat pump and solar photovoltaic system. *Energy*, *206*, Article 118091.

BP (2020). *BP energy outlook: 2020 edition.*

Cai, J., Zhang, F., & Ji, J. (2020). Comparative analysis of solar-air dual source heat pump system with different heat source configurations. *Renewable Energy*, *150*, 191–203.

Cai, J., Zhou, H., Xu, L., et al. (2021). Experimental and numerical investigation on the heating performance of a novel multi-functional heat pump system with solar-air composite heat source. *Sustainable Cities and Society*, *73*, Article 103118.

Chen, X., Zhang, S., & Ruan, S. (2021). Polycentric structure and carbon dioxide emissions: Empirical analysis from provincial data in China. *Journal of Cleaner Production*, *278*, Article 123411.

Cheon, S. -Y., Lim, H., & Jeong, J. -W. (2019). Applicability of thermoelectric heat pump in a dedicated outdoor air system. *Energy*, *173*, 244–262.

China Meteorological Administration Meteorological Data Center (2022). *China Meteorological Administration Meteorological Data Center.*

China Report (2022). *China Report: 75th Session of the United Nations General Assembly.*

Deng, M., Ma, R., Lu, F., et al. (2021). Techno-economic performances of clean heating solutions to replace raw coal for heating in Northern rural China. *Energy and Buildings*, *240*, Article 110881.

Dong, J., Zhang, L., Deng, S., et al. (2018). An experimental study on a novel radiant-convective heating system based on air source heat pump. *Energy and Buildings*, *158*, 812–821.

Dong, Z., Boyi, Q., Pengfei, L., et al. (2021). Comprehensive evaluation and optimization of rural space heating modes in cold areas based on PMV-PPD. *Energy and Buildings*, *246*, Article 111120.

Girard, A., Gago, E. J., Muneer, T., et al. (2015). Higher ground source heat pump COP in a residential building through the use of solar thermal collectors. *Renewable Energy*, *80*, 26–39.

Guo, X., & Goumba, A. P. (2018). Air source heat pump for domestic hot water supply: Performance comparison between individual and building scale installations. *Energy*, *164*, 794–802.

IEA (2020). *World energy outlook 2020.*

IEA (2020). *Renewables 2020 - Analysis and forecast to 2025.*

Latorre-Biel, J. -I., Jimémez, E., García, J. L., et al. (2018). Replacement of electric resistive space heating by an air-source heat pump in a residential application. Environmental amortization. *Building and Environment*, *141*, 193–205.

Li, S., Gong, G., & Peng, J. (2019). Dynamic coupling method between air-source heat pumps and buildings in China's hot-summer/cold-winter zone. *Applied Energy*, *254*, Article 113664.

Liu, M., He, Y., Zhang, H., et al. (2020). The feasibility of solar thermal-air source heat pump water heaters in renewable energy shortage regions. *Energy*, *197*, Article 117189.

Long, J., Xia, K., Zhong, H., et al. (2021). Study on energy-saving operation of a combined heating system of solar hot water and air source heat pump. *Energy Conversion and Management*, *229*, Article 113624.

Olsthoorn, D., Haghighat, F., Moreau, A., et al. (2017). Abilities and limitations of thermal mass activation for thermal comfort, peak shifting and shaving: a review. *Building and Environment*, *118*, 113–127.

Pinamonti, M., & Baggio, P. (2020). Energy and economic optimization of solar-assisted heat pump systems with storage technologies for heating and cooling in residential buildings. *Renewable Energy*, *157*, 90–99.

Rastegarpour, S., Gros, S., & Ferrarini, L. (2020). MPC approaches for modulating air-to-water heat pumps in radiant-floor buildings. *Control Engineering Practice*, *95*, Article 104209.

Shao, S., Zhang, H., Fan, X., et al. (2021). Thermodynamic and economic analysis of the air source heat pump system with direct-condensation radiant heating panel. *Energy*, *225*, Article 120195.

State Administration for Market Regulation (2020). *General rules for calculation of the comprehensive energy consumption, GB/T 2589-2020.*

Stetiu, C. (1999). Energy and peak power savings potential of radiant cooling systems in US commercial buildings. *Energy and Buildings*, *30*(2), 127–138.

Wang, Z., Li, G., Wang, F., et al. (2020). Techno-economic evaluation of a frost-free air source heat pump water heater. *Sustainable Cities and Society*, *57*, Article 102102.

Wu, P., Wang, Z., Li, X., et al. (2020). Energy-saving analysis of air source heat pump integrated with a water storage tank for heating applications. *Building and Environment*, *180*, Article 107029.

Xiong, Y., Liu, J., & Kim, J. (2019). Understanding differences in thermal comfort between urban and rural residents in hot summer and cold winter climate. *Building and Environment*, *165*, Article 106393.

Xu, W., Liu, C., Li, A., et al. (2020). Feasibility and performance study on hybrid air source heat pump system for ultra-low energy building in severe cold region of China. *Renewable Energy*, *146*, 2124–2133.

Xu, X., Wang, S., Wang, J., et al. (2010). Active pipe-embedded structures in buildings for utilizing low-grade energy sources: A review. *Energy and Buildings*, *42*(10), 1567–1581.

Yu, M., Li, S., Zhang, X., et al. (2021). Techno-economic analysis of air source heat pump combined with latent thermal energy storage applied for space heating in China. *Applied Thermal Engineering*, *185*, Article 116434.

Zhang, H., Jiang, L., Zheng, W., et al. (2019). Experimental study on a novel thermal storage refrigerant-heated radiator coupled with air source heat pump heating system. *Building and Environment*, *164*, Article 106341.

Zhang, L., Dong, J., Deng, S., et al. (2020). An experimental study on the starting characteristics of an improved radiant-convective air source heat pump system. *Energy and Buildings*, *226*, Article 110384.

Zhang, Q., Zhang, L., Nie, J., et al. (2017). Techno-economic analysis of air source heat pump applied for space heating in northern China. *Applied Energy*, *207*, 533–542.

Zhang, Y., Ma, Q., Li, B., et al. (2017). Application of an air source heat pump (ASHP) for heating in Harbin, the coldest provincial capital of China. *Energy and Buildings*, *138*, 96–103.